American Journal of Applied Sciences 2 (6): 1058-1064, 2005
ISSN 1546-9239

Increasing the Strength of Standard Involute Gear Teeth with Novel Circular Root Fillet Design

V. Spitas, Th. Costopoulos and C. Spitas
Laboratory of Machine Elements, Mechanical Engineering Department
National Technical University of Athens, Iroon Politechniou 9, 15780, Athens, Greece

Abstract: In this study the idea of spur gear teeth with circular instead of the standard trochoidal root fillet is introduced and investigated numerically using BEM. The strength of these new teeth is studied in comparison with the standard design by discretizing the tooth boundary using isoparametric Boundary Elements. In order to facilitate the analysis the teeth are treated as non-dimensional assuming unitary loading normal to the profile at their Highest Point of Single Tooth Contact (HPSTC), so that non-dimensional stress vs. Contact ratio diagrams are plotted. The analysis demonstrates that the novel teeth exhibit higher bending strength (up to 70%) in certain cases without affecting the pitting resistance since the geometry of the load carrying involute is not changed. The circular fillet design is particularly suitable in gear with a small number of teeth (pinions) and these novels gears can replace their existing counterparts in any mechanism without any alterations. Finally the geometry of the generating tool (i.e. rack) is determined in order to be able to cut these teeth using a generating method (i.e. hobbing).

Key words: Spur gears, circular fillet, root stress, generating rack, BEM

INTRODUCTION

In the field of gear transmissions there is a growing need for higher load carrying capacities and increased fatigue life. In order to achieve this, researchers focus either on the development of advanced materials (Hoffman *et al*.[1]) and new methods of heat treatment (Townsend and Bambeger[2], Legge[3], Herring[4]) or on the design of stronger tooth profiles (Litvin *et al*.[5], Tsai and Tsai[6]) and methods of gear manufacturing (Daniewicz and Moore[7]). However, in modern gear practice and manufacturing the majority of gear applications are covered by the standard 20^o involute teeth generated by rack, hob or CNC cutting process. This has a number of important advantages such as that of interchangeability, insensitivity to changes in the nominal center distance, commercial availability and easy manufacturing by conventional methods (i.e. hobbing) (Townsend[8]). On the other hand it has some disadvantages, one of which is that for a small number of teeth (practically less than 17 or 14 depending on the tip radius of the hob) the standard involute presents the problem of undercutting. In undercutting the tooth fillet is generated as the tip of the cutter removes material from the involute profile (generated previously by the straight part of the cutter), thus resulting in teeth that have a smaller thickness near their root, where the critical section is usually located (Townsend[8], Niemann[9]). In order to cope with this weakening of the gear teeth many solutions have been proposed (Fredette and Brown[10], Ciavarella and Demelio[11]) but the most commonly employed method is that of positive profile shifting (ISO 6336[12], AGMA 2101[13], Mabie *et al*.[14], Rogers *et al*.[15]) resulting in teeth with no undercutting, enhanced fatigue characteristics and changes in the nominal center distance of the gear pair. On the other hand these modified teeth exhibit lower pitting and scoring resistance and lower contrast ratio resulting in more noise and vibration during operation (Niemann[9]).

In the present study a novel design of fillet for spur gear teeth is presented. The proposed new teeth are composed of a standard involute working profile from the outer to the form circle of the gear and of a circular fillet profile from the form of the root circle of the gear replacing the conventional trochoidal fillet profile. These teeth are first modeled geometrically and then their behavior in bending is studied by assuming loading at their Highest Point of Single Tooth Contact (HPSTC). The maximum fillet stresses are calculated from various numbers of teeth using Boundary Element Analysis and the results are compared with the maximum fillet stress values of the corresponding standard teeth.

In order to facilitate the modelling and the analysis of these gears, their geometrical characteristics are normalized with respect to the module and the width of the gear and their loading characteristics, which depend

Corresponding Author: Th. Costopoulos, Laboratory of Machine Elements, Mechanical Engineering Department
National Technical University of Athens, Iroon Politechniou 9, 15780, Athens, Greece
E-mail: cost@central.ntua.gr

on the magnitude of the exerted load and its position at the Highest Point of Single Tooth Contact (HPSTC) on the flank, are normalized with respect to the magnitude of the load itself and the contrast ratio of the pair respectively. Therefore the tooth loading problem can be solved for these normalized "non-dimensional" teeth and then using simple linear relationships the stresses for the actual working tooth can be derived.

Another problem related to the capability of producing these novel teeth on conventional machines using standard generating-type methods for gear tooth cutting (i.e. Hobbing or rack-cutting) is investigated at the end of this study. The geometry of the generating rack with known geometry of the gear is calculated using the Theory of Gearing[16].

Non-dimensional gear tooth modelling: Consider the pair of spur gears schematically illustrated in Fig. 1 and denoted as 1 (driving) and 2 (driven). The law of gearing[8] requires that these gears should have the same nominal pressure angle a_o and the same module m in order to be able to mesh properly. It is also possible that these gears have addendum modifications x_1, x_2 respectively and therefore their pitch thickness is given by the following relationship:

$$s_{oi} = c_{si} \cdot \pi \cdot m + 2x_i \tan\alpha_o \cdot m = s_{oiu} \cdot m \qquad (1)$$

where c_{si} is the thickness coefficient of gear i,(i = 1,2), which in the general case is $c_{s1} \neq 0.5 \neq c_{s2}$, while s_{oiu} is the pitch thickness of the corresponding non-dimensional gear for which the module (m) and the face width (b) are both equal to unity.

Provided that no errors exist, the center distance O_1O_2 is calculated:

$$a_{12} = \frac{z_1 + z_2}{2} \cdot m + (x_1 + x_2) \cdot m = a_{12u} \cdot m \qquad (2)$$

The actual working pitch circle r_{bi} of gear i,(i = 1,2) should verify the law of gearing and therefore be equal to:

$$r_{bi} = \frac{z_i}{z_1 + z_2} \cdot a_{12u} \cdot m = r_{biu} \cdot m \qquad (3)$$

Let us now consider that gears 1 and 2 revolving about their centers O_1 and O_2 respectively are meshing along the path of contact AB illustrated in Fig. 1. During meshing there are two pairs of gear teeth in contact along the segments AA' and BB', thus sharing the total normal load, while there is only a single such pair when the tooth contact takes place along the central region A'B', carrying the total normal load. Point B' is the Highest Point of Single Tooth Contact (HPSTC) for gear 1 and its position, defining the radius $r_{B'}$, is (Spitas[17]):

$$r_{B'} = O_1B' = \sqrt{r_{k1}^2 + (\varepsilon - 1) \cdot t_g \cdot \left[(\varepsilon - 1) \cdot t_g - 2\sqrt{r_{k1}^2 - r_{g1}^2} \right]} \qquad (4)$$

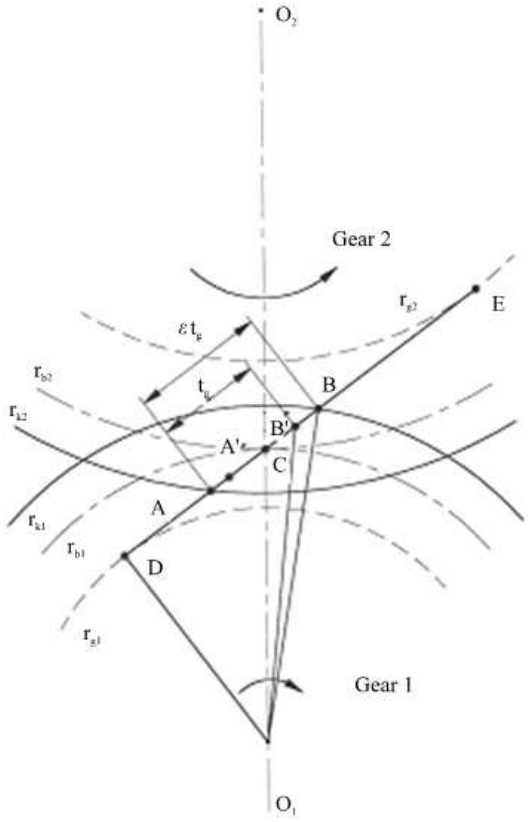

Fig. 1: Path of contact

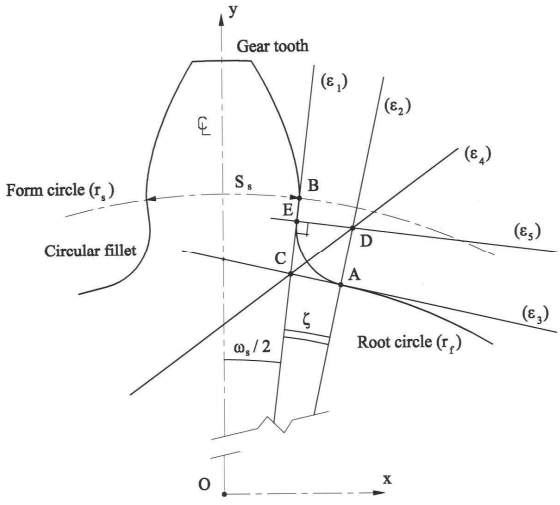

Fig. 2: The geometry of the circular fillet

and by dividing with the module of the pair, the above equation yields in terms of non-dimensional values:

$$r_{B'u} = \frac{r_{B'}}{m} = \sqrt{r_{k1u}^2 + (\varepsilon - 1)\cdot t_{gu}\cdot\left[(\varepsilon - 1)\cdot t_{gu} - 2\sqrt{r_{k1u}^2 - r_{g1u}^2}\right]} \quad (5)$$

From the above equation it is evident that the position of the HPSTC of a gear depends only on its geometry and on the contact ratio of the pair, in which all the characteristics of the mating gear are incorporated in a condensed form.

The advantage offered by this approach is profound, since the mechanical behavior of every gear can be modeled only by using its own geometrical characteristics z, x, cs and the contrast ratio ε of the pair (4 variables) instead of using all of the geometrical characteristics of the mating gear (6 variables). Also the use of non-dimensional teeth further simplifies the problem as every geometrical feature f on the transverse section of a full scale gear tooth is connected to the corresponding feature f_u of the transverse section of the non-dimensional gear tooth through the equation:

$$f = f_u.m \quad (6)$$

Stresses can also be calculated in non-dimensional teeth σ_u (z, x, Cs, ε) with unit loading $P_{Nu} = 1$ and related to the actual stress σ using the following equation:

$$\sigma = \sigma_u \cdot \frac{P_N}{b\cdot m} \quad (7)$$

as suggested by Rogers[15] and Townsend[8].

Geometrical modeling: Consider the involute spur gear tooth of circular fillet illustrated in Fig. 2 where point O is the center of the gear, axis Oy is the axis of symmetry of the tooth and point B is the point where the involute profile starts (from the form circle r_s).

A is the point of tangency of the circular fillet with the root circle r_f. Point D lying on $(\varepsilon_2) \equiv OA$ represents the center of the circular fillet. Line (ε_3) is tangent to the root circle at A and intersects with the line (ε_1) at C. The fillet is tangent to the line (ε_1) at point E. Since it is always $r_s > r_f$ (Townsend[8]), the proposed circular fillet can be implemented without exceptions on all spur gears irrelevant of number of teeth or other manufacturing parameters. A comparison of the geometrical shape of a tooth of circular fillet with that of standard fillet is presented in Fig. 3.

For the geometric modeling only dimensionless teeth are examined i.e. teeth with unit module (m) and face width (b). In dimensionless teeth the pitch radius and the pitch thickness are calculated:

$$r_o = \frac{z}{2} \text{ and } S_{ov} = \pi\cdot c_s + 2x\cdot\tan\alpha_o$$

$$S_s = r_s\cdot\left[\frac{S_{ov}}{r_o} + 2\left(\phi_o - \phi_s\right)\right] \quad (8)$$

where:

$\phi_s = \tan\alpha_s - \alpha_s$ is the involute function on circle r_s

$\alpha_s = \cos^{-1}\frac{r_g}{r_s}$ is the pressure angle on circle r_s

Angle $\omega_s/2$ that corresponds to the arc $S_s/2$ (Fig. 2) is given by the equation:

$$\omega_s/2 = \frac{S_s/2}{r_s} = \Omega_s \quad (9)$$

Angle ζ (Fig. 2) takes values between 0 and ζ_{max} so that:

$$\zeta_{max} = \frac{\pi}{z} - \Omega_s \quad (10)$$

The coordinates of points A and B are:

$$x_A = r_f\sin\left(\zeta + \Omega_s\right),\ y_A = r_f\cos\left(\zeta + \Omega_s\right) \quad (11)$$

$$x_B = r_f\sin\Omega_s,\ \ y_B = r_f\cos\Omega_s \quad (12)$$

The defining equations of lines (ε_1) and (ε_2) are respectively:

$$(\varepsilon_1): y = \frac{1}{\tan\Omega_s}\cdot x,\ (\varepsilon_2): y = \frac{1}{\tan\left(\zeta + \Omega_s\right)}\cdot x \quad (13)$$

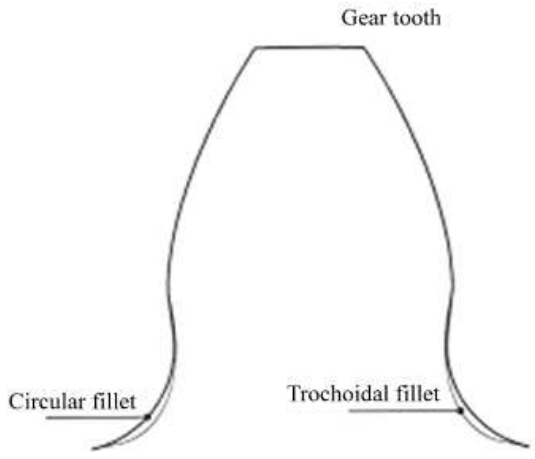

Fig. 3: Superposition of circular fillet on a standard tooth

Since $(\varepsilon_3)\perp(\varepsilon_2)$ and (ε_3) passes through point $A(x_A, y_A)$ its defining equation is.

Point $C(x_C, y_C)$ is the intersection of (ε_1) and (ε_3) and therefore its coordinates should verify eq. (13) and hence:

$$x_C = r_f \cdot \frac{\tan\Omega_s}{\sin(\zeta+\Omega_s)\tan\Omega_s + \cos(\zeta+\Omega_s)} \quad (14)$$

$$y_C = \frac{x_C}{\tan\Omega_s} \quad (15)$$

Angle $B\hat{C}A$ is calculated as:

$$B\hat{C}A = \left(\frac{\pi}{2}-\Omega_s\right)+\zeta+\Omega_s = \frac{\pi}{2}+\zeta \quad (16)$$

Line (ε_4) bisects the previous angle $B\hat{C}A$, so its inclination is:

$$\tan\left[\frac{B\hat{C}A}{2}-(\zeta+\Omega_s)\right] = \tan\left(\frac{\pi}{4}-\frac{\zeta}{2}-\Omega_s\right) \quad (17)$$

Point $C(x_C, y_C)$ belongs to (ε_4) and thus the defining equation of the line (ε_4) is derived as:

$$y = \tan\left(\frac{\pi}{4}-\frac{\zeta}{2}-\Omega_s\right)x + r_f \cdot \frac{1-\tan\Omega_s\tan\left(\frac{\pi}{4}-\frac{\zeta}{2}-\Omega_s\right)}{\sin(\zeta+\Omega_s)\tan\Omega_s+\cos(\zeta+\Omega_s)} \quad (18)$$

At this point two distinct cases are considered.

Point E coincides with point B(E≡B): In this case $(\varepsilon_5)\perp(\varepsilon_1)$ at point E ≡ B, so (ε_5) must have an inclination equal to $-\tan\Omega_s$ and since point B belongs to (ε_5) its defining equation is:

$$y = -\tan\Omega_s \cdot x + \frac{r_s}{\cos\Omega_s} \quad (19)$$

Point $D(x_D,y_D)$ should verify both eqs. (13) and (19) and therefore has the following coordinates:

$$x_D = r_s \cdot \frac{\tan(\zeta+\Omega_s)}{\cos\Omega_s+\sin\Omega_s\tan(\zeta+\Omega_s)}$$

$$y_D = r_s \cdot \frac{1}{\cos\Omega_s+\sin\Omega_s\tan(\zeta+\Omega_s)} \quad (20)$$

According to Fig. 2 it is AC=BC and after substitutions and calculations we arrive at the equation:

$$\frac{r_f^2+r_s^2}{2} = \frac{r_s r_f}{\cos\zeta}\cdot\left(\sin^2\Omega_s+\cos^2\Omega_s\right) \quad (21)$$

from which the value of ζ is derived as:

$$\zeta = \cos^{-1}\frac{2r_s r_f}{r_s^2+r_f^2} \quad (22)$$

By defining the dimensions parameter $S = \frac{r_s}{r_f} > 1$ eq. (22) becomes:

$$\zeta = \cos^{-1}\left(\frac{2S}{1+S^2}\right) \quad (23)$$

Equation (23) is used for the determination of the angle (ζ).

Point E lies below point B: In this case it is $\zeta \le \zeta_{max}$ and the center of the circular fillet of the tooth is calculated following the methodology described below:

$$CA = \sqrt{(x_A-x_C)^2+(y_A-y_C)^2} = CE \quad (24)$$

$$AD = CA\cdot\tan\left(\frac{\pi}{4}+\frac{\zeta}{2}\right) \quad (25)$$

The coordinates of points $D(x_D,y_D)$ and $E(x_E,y_E)$ are respectively:

$$x_D = (r_f+AD)\sin(\zeta+\Omega_s),\quad y_D = (r_f+AD)\cos(\zeta+\Omega_s) \quad (26)$$

$$x_E = (OC+CE)\sin\Omega_s,\quad y_E = (OC+CE)\cos\Omega_s \quad (27)$$

The remaining portion of the tooth profile between points B and E is a straight line.

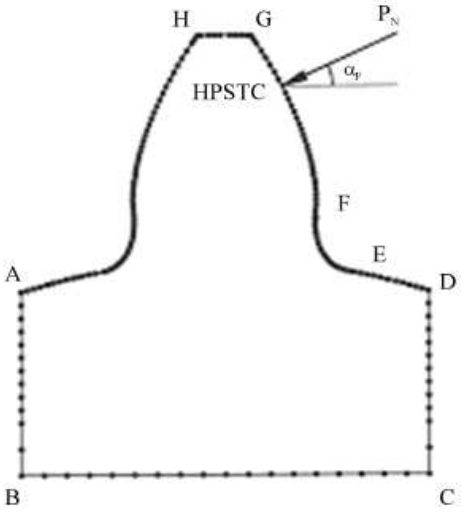

Fig. 4: BEM mesh on a tooth model

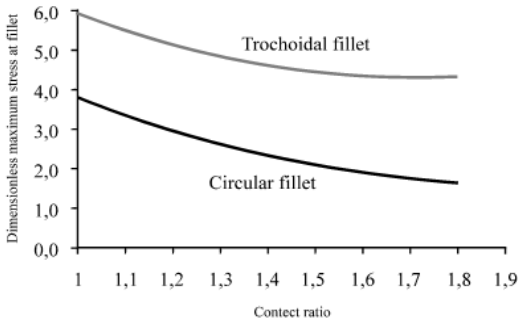

Fig. 5: Non-dimensional stresses for a gear with 9 teeth

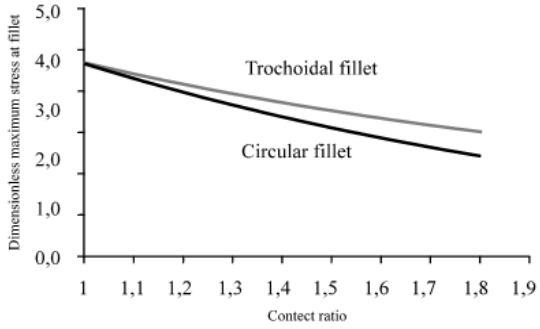

Fig. 6: Non-dimensional stresses for a gear with 32 teeth

Structural modeling: The structural analysis of the spur gear tooth model is carried out using the Boundary Element method with quadratic isoparametric boundary elements. The calculation of the non-dimensional tooth profile and the generation of the mesh are done automatically using specially developed software. The normal load is exerted at its Highest Point of Single Tooth Contact (HPSTC) and again it is considered to be unitary (i.e. $P_N = 1$). The resultant normalized stress is related to the actual stress of the full-scale tooth with eq. (7). The distance of the HPSTC from the center of the gear is calculated in terms of the contrast ratio ε and the geometrical characteristics of the gear according to eq. (4)

A typical mesh is presented in Fig. 4. The tooth base, ABCD, is discretized in 43 nodes or 21 elements and is considered to be fixed, i.e. The displacements of all nodes are zero.

Portion DE represents the root circle and is discretized in 11 nodes or 5 elements. Portion EF is the tooth fillet consisting of 72 elements or 144 nodes, portion FG is the involute part of the tooth consisting of 40 elements or 81 nodes and finally a portion GH is the tip, discretized in 5 elements or 11 nodes. All nodes belonging to the tooth profile are considered to be unloaded (horizontal and vertical traction equal to zero) with the exception of the node marked HPSTC, which belongs to the involute part FG and on which the normal load P_N is acting.

The reason that the mesh is denser at the tooth fillet is that the maximum stress is expected to occur at this area and therefore greater density will ensure increased accuracy of the results (both the position of the critical section and the magnitude of the maximum developed stress).

RESULTS AND DISCUSSION

A comparative study has been carried out between the structural properties of the standard trochoidal filleted teeth generated by hobbing and the proposed circular filleted involute teeth. Five distinct cases have been examined for unshifted teeth with 9, 17, 24, 32 and 40 teeth respectively. These teeth were considered to be dimensionless and loaded at their Highest Point of Single Tooth Contact (HPSTC). Since the HPSTC for a given gear pair depends only on the geometrical characteristics of the gear and on the contact ratio of the pair, stress versus contact ratio diagrams are plotted. All gears were thoroughly examined for interference during meshing and it has been proved that there is no such danger when replacing the standard trochoidal fillet with the novel circular fillet.

In Fig. 5 the effect of the new design to a gear with a small number of teeth is investigated. A gear with only 9 teeth presents severe undercutting and is of little practical use unless it is shifted by a substantial amount. However by doing so the contrast ratio of the pair becomes smaller and the hertzian contact stresses rise thus reducing its pitting resistance. By introducing the concept of the circular fillet it can be seen that its fatigue resistance is increased by 25.26% for tip loading (ε=1. 0) and up to 68.90% for ε=1. 8 without affecting the contact pressure.

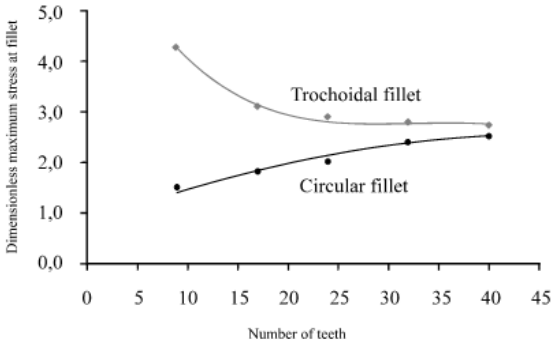

Fig. 7: Comparison between the new and the standard design for ε = 1.6

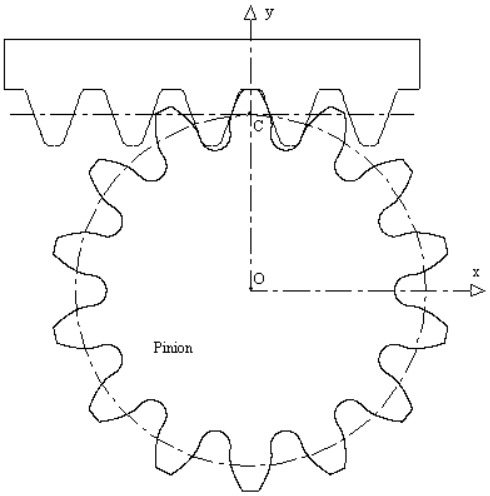

Fig. 8: Generating rack/pinion with circular fillet

In Fig. 6 a gear with 32 teeth is examined. Here it is evident that the differences between the new and the existing design are less important as the maximum decrease of the bending stress is only 20% for ε = 1.8.

In all cases the new circular fillet design is found better than the standard one and this is more evident as the number of teeth decreases or as the HPSTC moves lower towards the pitch circle. As the number of teeth increases the difference between the two designs becomes smaller and tends to be asymptotically zero when the number of teeth gets tends to infinity as in the case of a rack, where even the standard design gives a circular fillet. This effect is illustrated in Fig. 7, where the maximum stress versus the number of teeth is plotted for a usual gear pair with HPSTC corresponding to a contact ratio of 1.6.

The proposed fillet geometry has another advantage compared to other non-generated gear tooth forms since it can be cut on conventional hobbing machines or rack-cutting machines without the need of special tooth number-specific milling tools.

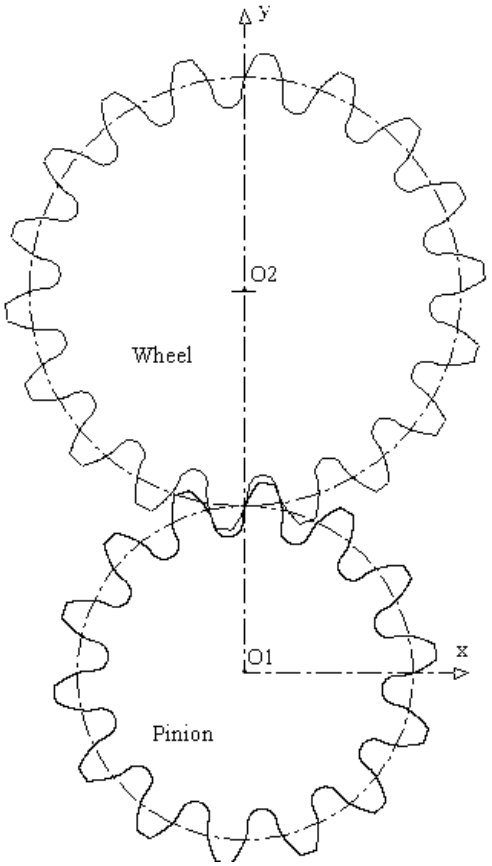

Fig. 9: Pinion-wheel pair with circular filleted teeth in mesh

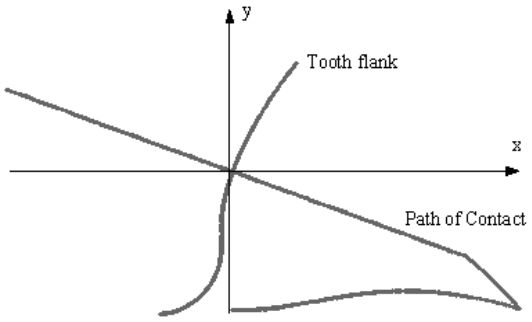

Fig. 10: Full path of contact of the gear tooth flank

The generating rack is only slightly different than the standard one only near its tip (which in turn generates the root fillet of the tooth). As it is usually pinions that undergo the higher bending stresses developed in the gear pair during meshing, the same generating rack can be used to cut the mating wheel teeth, although their root fillet geometry will not be strictly circular as for the pinion. Anyway the wheel teeth will also exhibit increased strength compared to the conventional ones generated with the standard circular tipped rack/hob.

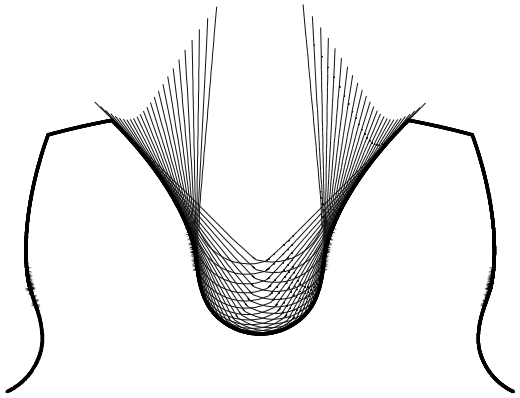

Fig. 11: Cutting process of the circular filleted teeth by the generating rack and creation of the enveloping surfaces

In Fig. 10 the full path of contact corresponding to a pinion tooth flank with circular filleted teeth is illustrated in detail. Note that the path of contact is composed of a straight linear part inclined at 20° to the horizontal at which the meshing and the power transmission between gears takes place and of a complicated reversing end part at which the cutting action (i.e. Meshing with the generating rack tooth) takes place.

Finally in Fig. 11 the cutting (generating) process of such a fillet is illustrated. Note that the straight part of the rack remains unchanged so in fact the novel teeth are still standard involute teeth retaining all the well known advantages of the involute.

CONCLUSIONS

The effect of the novel proposed circular fillet design on the bending stresses developed in spur gear teeth was investigated in comparison with the standard design. The new geometry incorporating the circular fillet was modeled for dimensionless teeth and the maximum bending stress was calculated using a BEM considering unit loading at the HPSTC of the tooth.

It was demonstrated that the novel circular design surpasses the existing trochoidal design of the spur gear tooth fillet in terms of fatigue endurance without affecting the pitting resistance. This is more evident on gears with a small number of teeth (i.e. Pinions with less than 30 teeth). The proposed geometry does not produce undercut teeth even for a small number of teeth and can be easily manufactured using standard involute hobbing tools with special tip design. Furthermore the novel fillets can be ground more easily due to their circular design even with conventional, easy to manufacture tools and thus increase the fatigue properties of the gear pair further.

REFERENCES

1. Hoffman, G. *et al*., 1999. Testing P/M Materials for High Loading Gear Applications. Intl. J. Powder Metallurgy, 35: 35-44.
2. Townsend, D.P. and E.N. Bambeger, 1991. Surface Fatigue Life of Carburized and Hardened M50NiL and AISI 9310 Spur Gears and Rolling Contact Test Bars. J. Propulsion and Power, Vol: 7.
3. Legge, G., 1988. Plasma Carburizing-Facility Design and Operation Data, Industrial Heating, pp: 26-30.
4. Herring, D.H., 1987. Why Vacuum Carburizing Is Effective for Today and Tomorrow: II, Industrial Heating, pp: 22-26.
5. Litvin, F.L., L. Qiming and A.L. Kapelvich, 2000. Asymmetrical Modified Spur Gear Drives: Reduction of Noise, Localization of Contact, Simulation of Meshing and Stress Analysis. Computer Methods in App. Mechanics and Eng., 188: 363-390.
6. Tsai, M. and Y. Tsai, 1998. Design of High Contact Ratio Spur Gears Using Quadratic Parametric Tooth Profiles. Mechanism and Machine Theory, 33: 551-564.
7. Daniewicz, S.R. and D.H. Moore, 1998. Increasing the bending Fatigue Resistance of Spur Gear Teeth Using a Presetting Process. Intl. J. Fatigue, 20: 537-542.
8. Townsend, D.P., 1992. Dudley's Gear Handbook-the design, manufacture and application of gears. McGraw-Hill, New York.
9. Niemann, G., 1965. Maschinenelemente. Band 2, Springer, Verlag.
10. Fredette, L. and M. Brown, 1997. Gear Stress Reduction Using Internal Stress Relief Features. J. Mechanical Design, 119: 518-521.
11. Ciavarella, M. and G. Demelio, 1999. Numerical Methods for the Optimization of Specific Sliding, Stress Concentration and Fatigue Life of Gears. Intl. J. Fatigue, 21: 465-474.
12. ISO, 6336-3, 1996. Calculation of the load capacity of spur and helical gears-Part 3. Calculation of tooth bending strength.
13. AGMA, 2101-C95, 1995. Fundamental rating factors and calculation methods for involute spur and helical gear. (Metric version). American Gear Manufacturers Association.
14. Mabie, H.H., C.A. Rogers and C.F. Reinholtz, 1990. Design of Nonstandard Spur Gears Cut by a Hob, Mechanism and Machine Theory, 25: 635-644.
15. Rogers, C.A., H.H. Mabie and C.F. Reinholtz, 1990. Design of Spur Gears Generated with Pinion Cutters. Mechanism and Machine Theory, 25: 623-634.
16. Litvin, F.L., 1994. Gear Geometry and Applied Theory. Prentice Hall, Englewood Cliffs, NJ.
17. Spitas, V.A. and T. Costopoulos, 2001. New Concepts in Numerical Modeling and Calculation of the Maximum Root Stress in Spur Gears versus Standard Methods: A Comparative Study. Proc. 1st National Conf. Recent Advances in Mechanical Eng., ASME-Greek Section, Patras.